SUPPORTING INFORMATION

Rational design of a conformation-specific antibody for the quantification of Aβ oligomers

Francesco A. Aprile, Pietro Sormanni, Marina Podpolny, Shianne Chhangur, Lisa-Maria Needham, Francesco S. Ruggeri, Michele Perni, Ryan Limbocker, Gabriella T. Heller, Tomas Sneideris, Tom Scheidt, Benedetta Mannini, Johnny Habchi, Steven F. Lee, Patricia C. Salinas, Tuomas P. J. Knowles, Christopher M. Dobson and Michele Vendruscolo

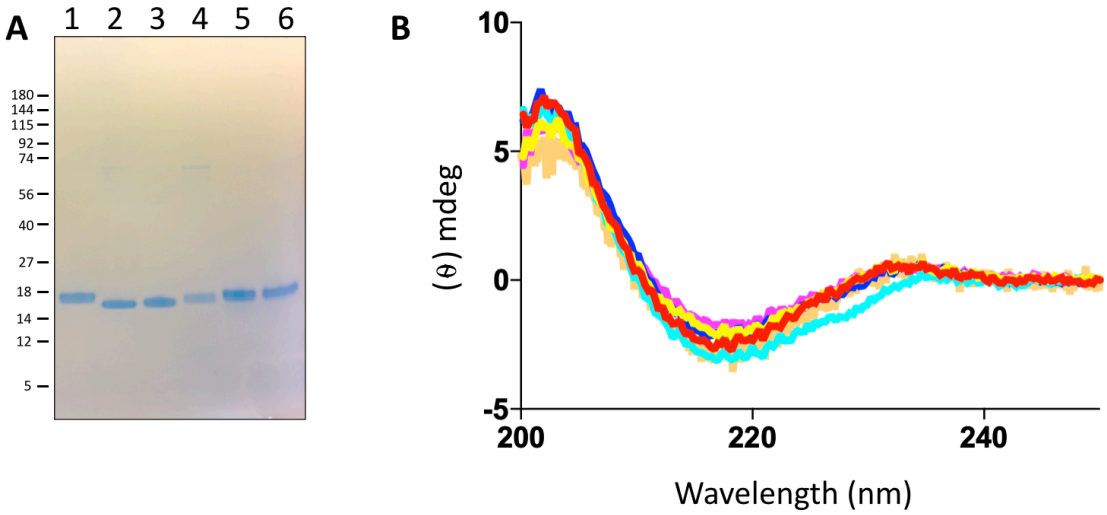

C

MRGSHHHHHHGMASMTGGQQMGRDLYDDDDKDPKLEVQLVESGGGLVQPGGS
LRLSCAASGFNIKDTYIGWVRRAPGKGEEWVASIYPTNGYTRYADSVKGRFTISA
DTSKNTAYLQMNSLRAEDTAVYYCAAGS**ESAFGRA**EEEAAAWGQGTLVTVSSGT

Figure S1. Characterisation of the DesAbs used in this work, as identified by their designed CDR3. (A) SDS-PAGE. Lane 1: PMSAIVS, lane 2: YHADISNE, lane 3: LEVIVRS, lane 4: ESAFGRA, lane 5: PYGSMYVHS, lane 6: GAVLTAK. **(B)** CD analysis. Red: PMSAIVS, yellow: YHADISNE, cyan: LEVIVRS, blue: ESAFGRA, magenta: PYGSMYVHS, orange: GAVLTAK. The molecular weights (in kDa) of the protein marker are shown on the left side of the gel. **(C)** Amino acid sequence of DesAb-O where the complementary peptide in the CDR3 is shown in bold.

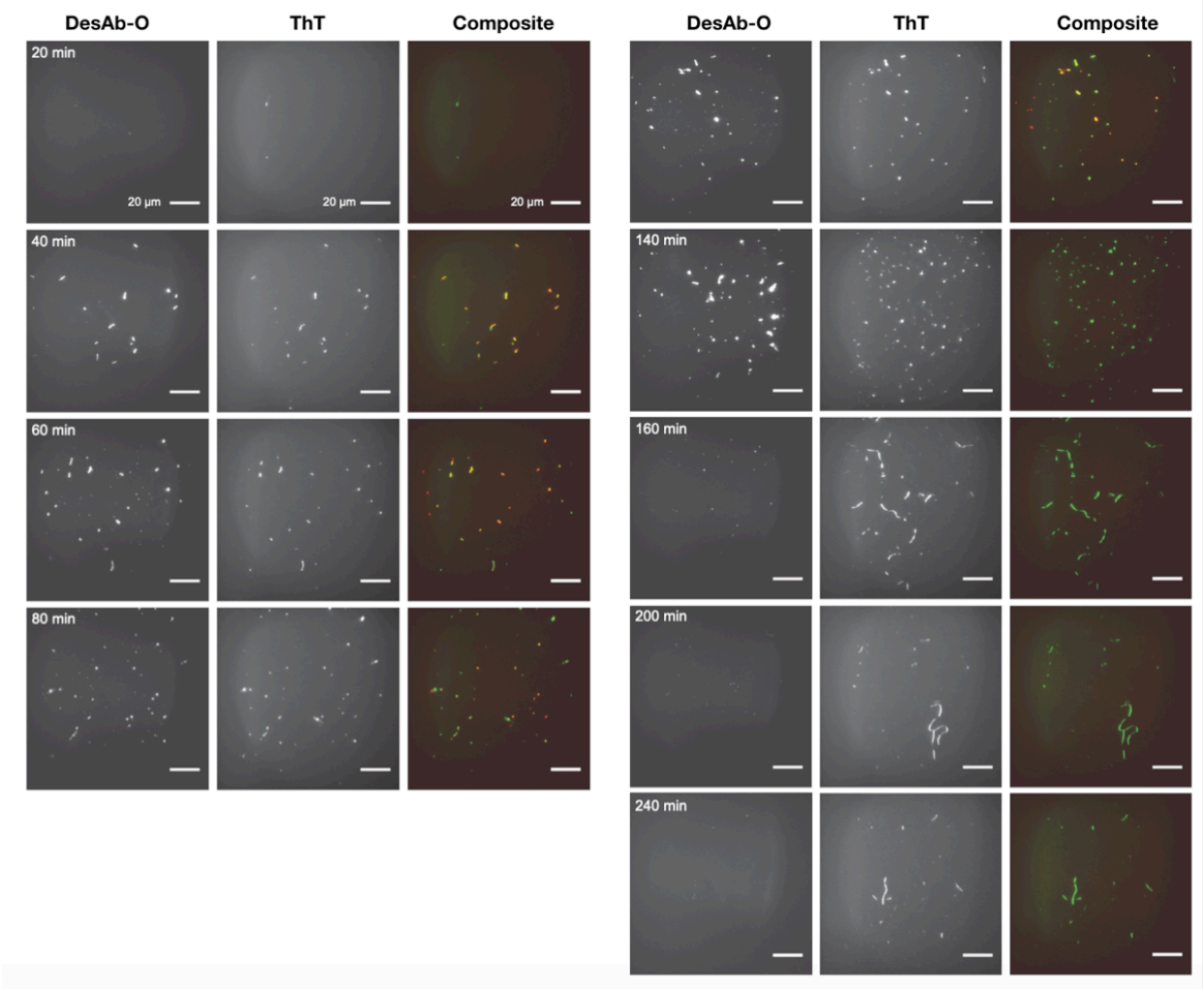

Figure S2. TIRF single particle analysis of aggregates from an aggregation reaction of Aβ42. TIRF microscopy images of different time points of the aggregation reaction. ThT, AF647 channels and composite images are shown. Bars indicate 20 µm.

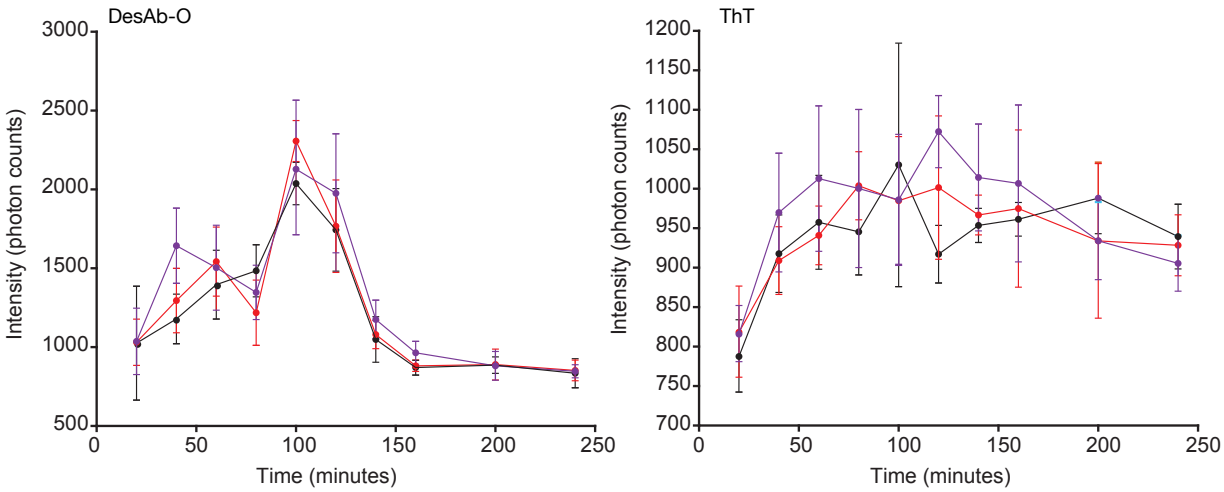

Figure S3. Time course of the fluorescence of DesAb-O-AF647 and ThT during the aggregation of Aβ42. Data gathered in the TIRF experiment and used for calculating the coincidence % shown in Fig. 2a. Three independent experiments are shown (black, red, violet). Each point is the average of 10 fields, where error bars represent the standard deviation of these fields.

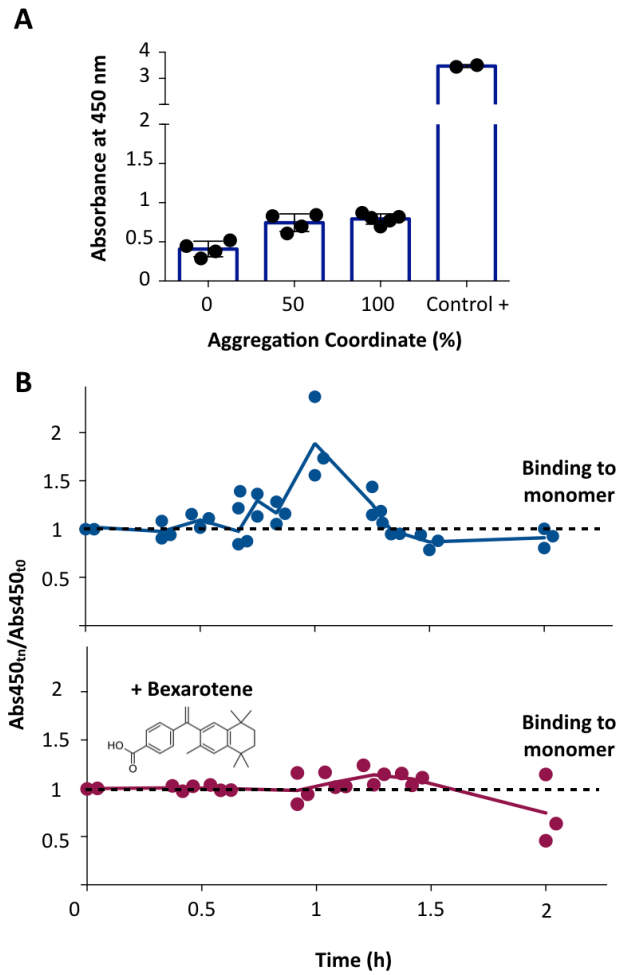

Figure S4. **(A)** Raw data corresponding to the ELISA plot with DesAb-Aβ$_{18\text{-}24}$ in Fig. 4d. A positive control is shown to demonstrate that the absorbance signal was not saturated. Error bars represent the standard deviation. **(B)** Plots showing individual data points from Fig. 3e.

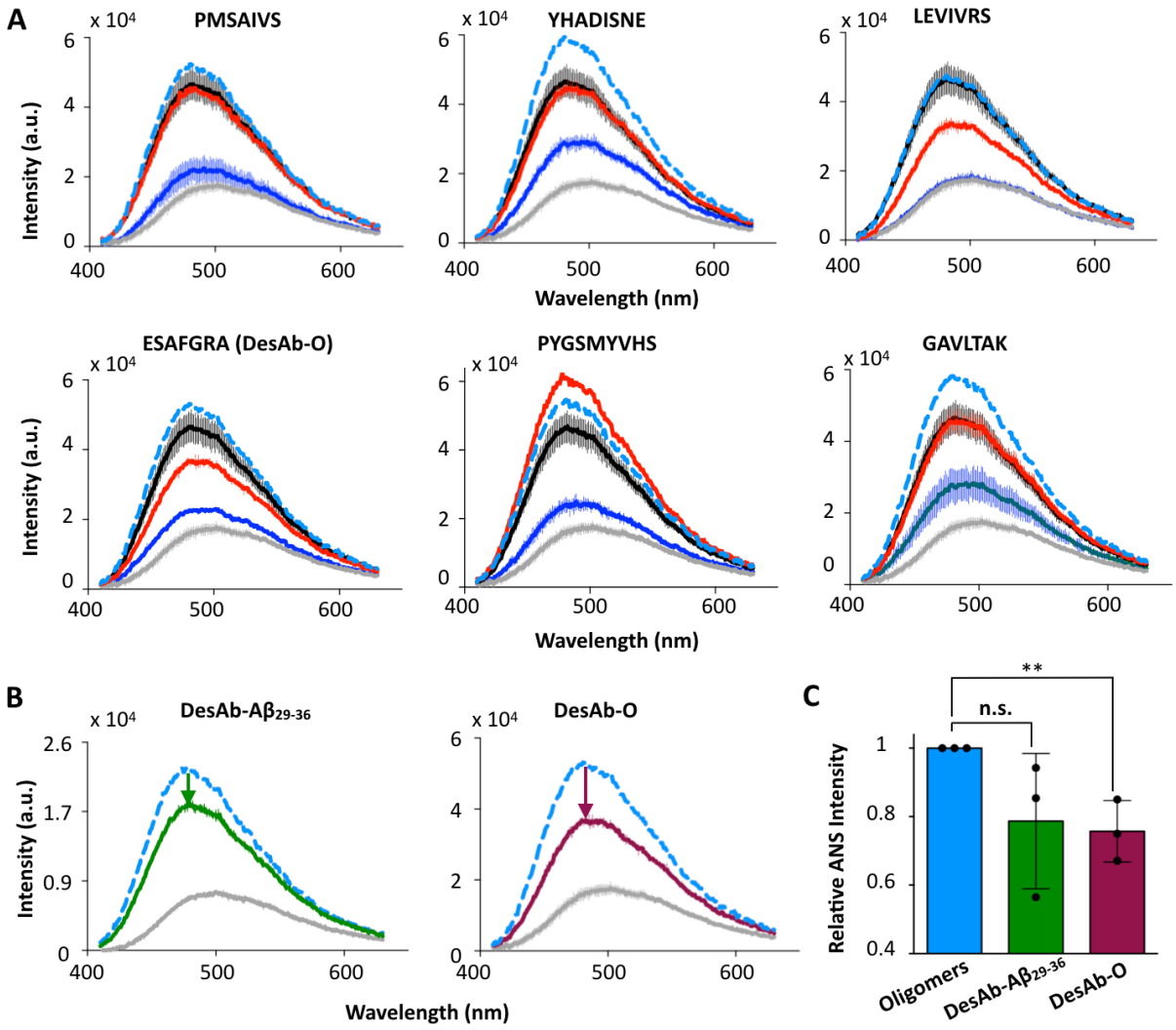

Figure S5. ANS binding assays of the DesAbs generated for this work. (A) For each DesAb (the designed CDR3 is indicated on the top of each graph), the fluorescence spectrum of ANS alone is reported in grey, of ANS in the presence of Aβ40 oligomers in black, of ANS in the presence of the DesAb in blue, of ANS with both oligomers and DesAb in red. The dashed cyan lines represent the expected spectrum for solutions with both oligomers and DesAbs given by the linear sum of the spectra obtained in the presence of oligomers alone and DesAbs alone. **(B)** ANS fluorescence spectra for characterising the binding of $DesAb_{29-36}$ and DesAb-O to Aβ40 oligomers. For each experiment, the fluorescence spectrum of ANS alone is reported in grey, of ANS in the presence of DesAbs and Aβ40 oligomers in green for $DesAb_{29-36}$ and in purple for DesAb-O. The dashed cyan lines represent the expected spectrum for solutions with both oligomers and DesAb in the case this spectrum was given by the linear sum of the spectra in the presence of oligomers alone and DesAbs alone (not

shown in this representation). The arrows show the decrease of the intensity peak upon addition of the corresponding antibody. In (A) and (B), experiments shown are representative of a total of three individual experiments. Each spectrum is the average of two individual replicates and the error bars represent the standard deviation. **(C)** Bar plot showing the relative ANS intensity of oligomers (cyan), $DesAb_{29-36}$ (green), and DesAb-O (purple). The relative ANS intensity was calculated as (ANS intensity *recorded* in the presence of DesAb)/ (ANS intensity *expected* in the presence of DesAb if the spectrum was given by the linear sum of the spectra obtained in the presence of oligomers alone and DesAb alone). Statistical analysis was performed by a t-test (C.I. 0.95; ** $P \leq 0.01$).

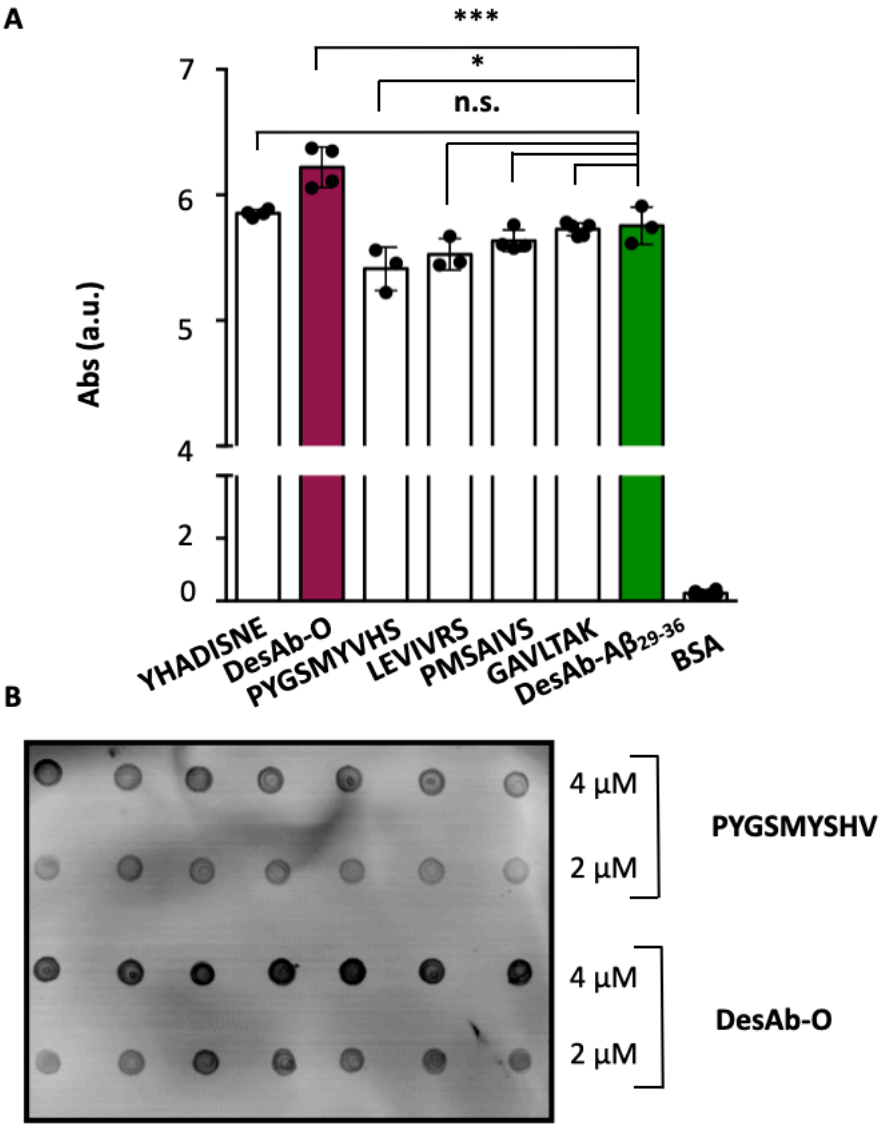

Figure S6. Assessment of the binding of the DesAbs to Aβ40 oligomers. **(A)** ELISA experiments performed to measure the binding of the DesAbs to Aβ40 oligomers. The DesAbs were loaded on the ELISA plate and then incubated in the presence of Aβ40 oligomer solutions. The bar corresponding to DesAb-O is coloured in magenta while the one corresponding to the original DesAb-$A\beta_{29\text{-}36}$ in green. Error bars represent the standard deviation. Statistical analysis was performed by ANOVA with multiple-comparison (C.I. 0.95; * $P \leq 0.05$, *** $P \leq 0.001$). **(B)** Dot-blot to determine the binding of DesAb-O to Aβ40 oligomers compared to the antibody with lowest affinity (CDR3: PYGSMYSHV), according to ANS binding assay. Also in this case, the DesAbs were first spotted on the membrane plate and then incubated in the presence of Aβ40 oligomer solutions.

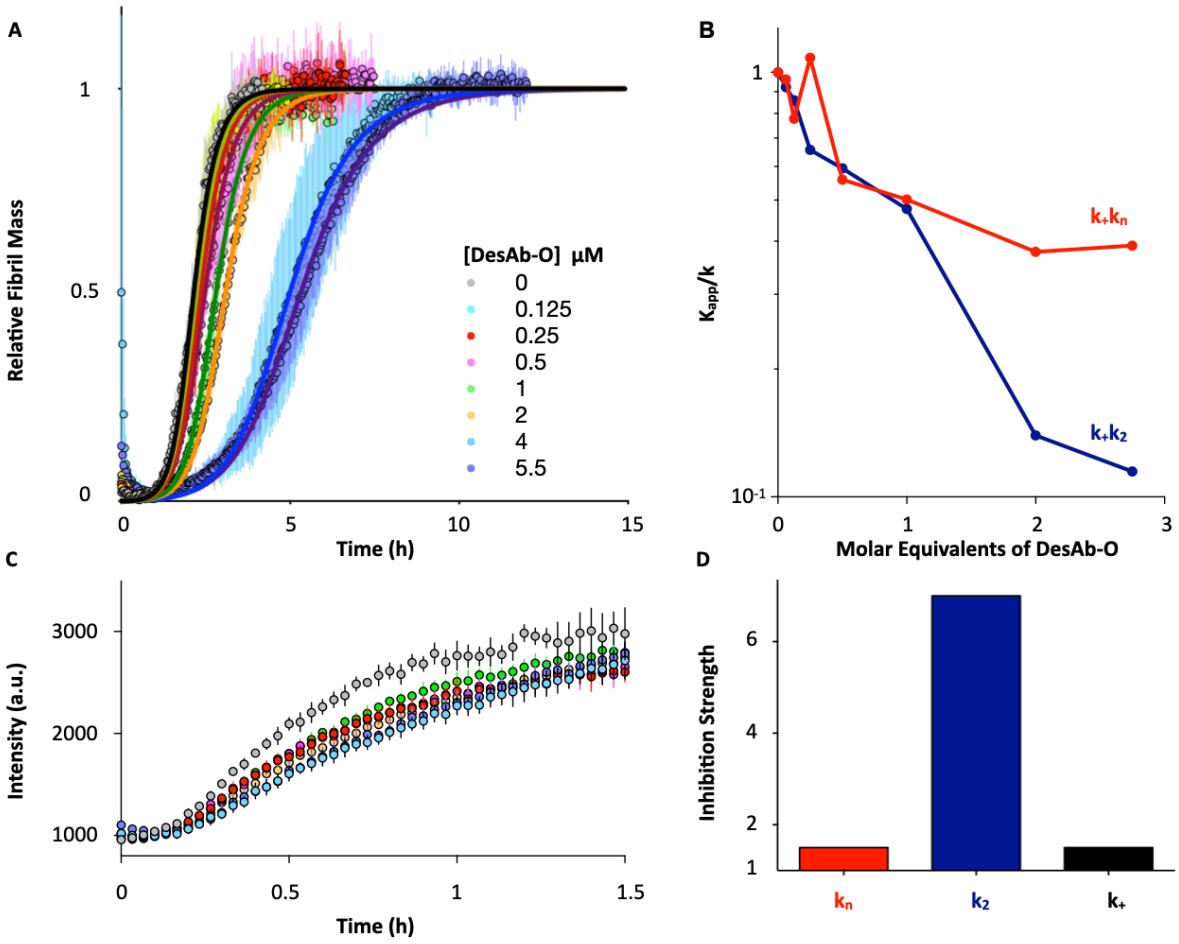

Figure S7. Analysis on the inhibition of Aβ42 aggregation by DesAb-O. (A) ThT aggregation experiments of 2 µM monomeric Aβ42 in the presence of different concentrations of DesAb-O. Data are reported as relative fibril mass (dots) and are the average of at least 3 individual replicates. **(B)** Decrease of the global parameters k_nk_+ (red) and k_2k_+ (blue) evaluated from the fit as a function of the relative antibody concentration shown in (A). **(C)** ThT aggregations experiments of 2 µM monomeric Aβ42 and 0.4 µM Aβ42 preformed fibrils in the presence of different concentrations of DesAb-O. Fluorescence values (dots) are the average of at least 5 individual replicates. Colours corresponds to concentrations as shown in A. **(D)** Bar plot of the inhibition strength of DesAb-O (defined as $k_{A\beta42}/k_{A\beta42+DesAb\text{-}O}$) on k_+ (black), k_n (red), and k_2 (blue) rate constants, derived from (A, B, C). Errors bars in (A) and (C) represent the standard deviation.

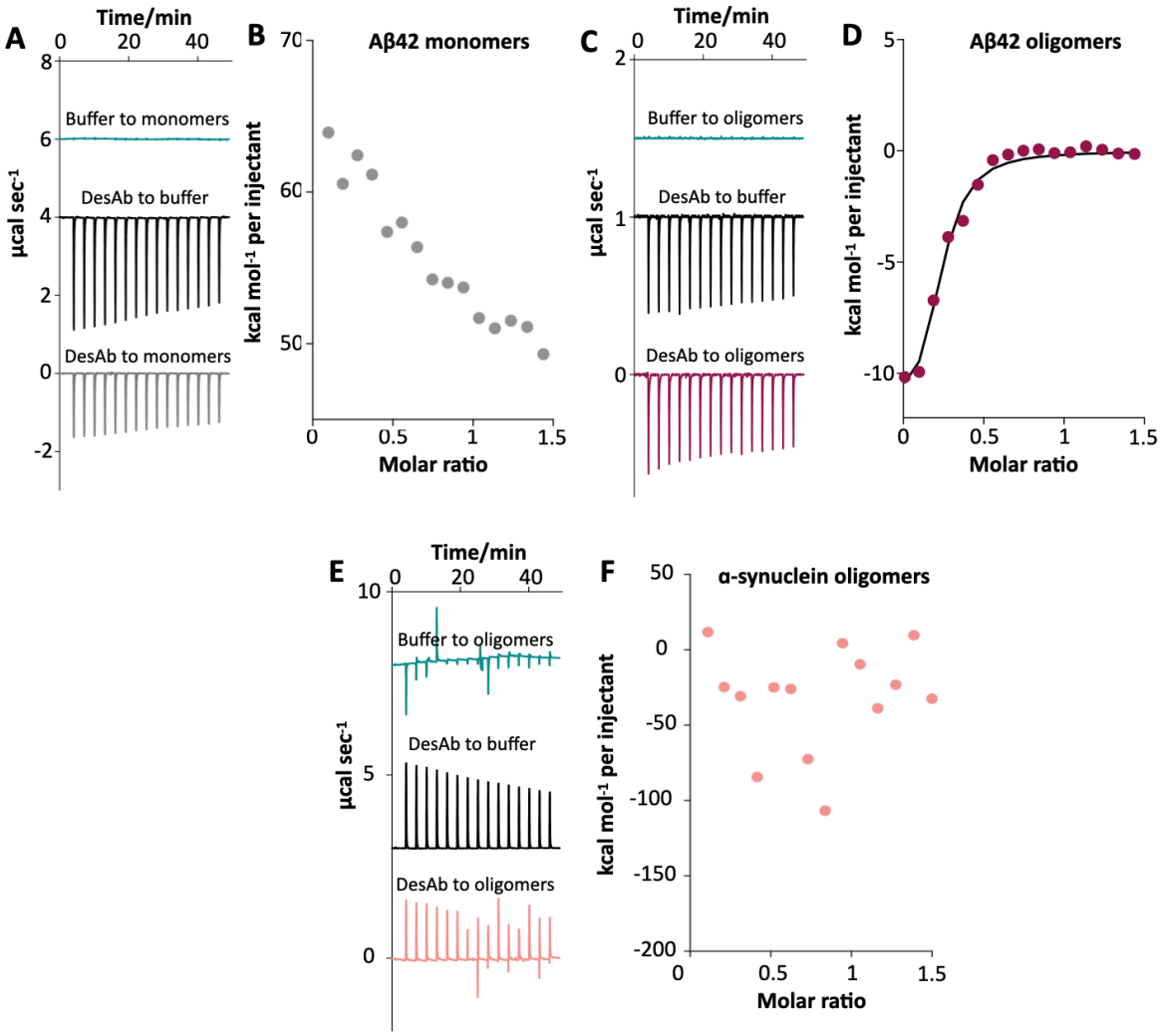

Figure S8. ITC experiments for measuring the binding of DesAb-O to Aβ40 monomers and oligomers, and to control α-synuclein oligomers. (A, B) Binding of DesAb-O to Aβ40 monomers. Solutions contain minimal amounts of DMSO to ensure that Aβ40 remains monomeric. Baseline corrected raw data are shown in panel A. Dilution controls were vertically shifted for visibility. Double subtracted integrated peaks are reported in panel B. **(C, D)** Binding of DesAb-O to Zn^{2+}-stabilised Aβ40 oligomers. Baseline corrected raw data are shown in panel C. Dilution controls were vertically shifted for visibility. The double subtracted integrated peaks and fit (black line) are shown in panel D. Values from fitting: K_d of 440 ± 1.5 nM; n= 4.8 ± 0.23; ΔH = -1.27E4 ±9.4E2 cal/mol; ΔS = -13.4 ±9.4E2 cal/mol/deg. **(E, F)** Binding of DesAb-O to control α-synuclein oligomers. Baseline corrected raw data are shown in panel E, while the double subtracted integrated peaks are reported in panel F.

Supplementary Movie Legends

Movie S1. dSTORM imaging of AF647-DesAb-O bound to Aβ42 collected at 40 minutes into the aggregation reaction.

Movie S2. dSTORM imaging of AF647-DesAb-O bound to Aβ42 collected at 140 minutes into the aggregation reaction.